

## Electric stresses Control on the Surface Contour of FGM Post Type Spacer with Delamination and Particle in a Three-Phase GIS

<sup>1</sup>**Pagidela Yamuna**, Assistant Professor (Adhoc), Department of EEE, JNTUACEP,  
yamuna.pagidela@gmail.com

<sup>2</sup>**K.Ravisankar**, Assistant Professor (Adhoc), Department of EEE, JNTUACEP, krs.sai@gmail.com

<sup>3</sup>**P.Janaki**, 1Assoc. Prof., Department of EEE, Lendi Institute of Engineering & Technology,  
janaki.pakalapati@gmail.com

<sup>4</sup>**N.Madhava Reddy**, Assistant Professor (Adhoc), Department of CIVIL, JNTUACEP,  
[nmmadhava136.ce@jntua.ac.in](mailto:nmmadhava136.ce@jntua.ac.in)

<sup>5</sup>**Vempalle Rafi**, Assistant Professor (Adhoc), Department of EEE, JNTUACEP, vempallerafi@gmail.com

### Abstract

Gas Insulated Busduct (GIB) is the most preferred choice for high voltage (HV) applications to meet the power demand. The switching operations and manufacturing process can result in various flaws, such as delamination, protrusion, depression, void, etc., which lead to insulator failures in GIBs. These defects have a significant negative impact on the distribution of the field along the length of the spacer, which de-energizes the entire GIB system and causes a significant economic loss. A spacer of post type with Functionally Graded Material (FGM) is designed in this paper for a 3-phase GIB under delamination to mitigate the electric stresses along the length of the spacer. Aluminium oxide (Al<sub>2</sub>O<sub>3</sub>), Titanium dioxide (TiO<sub>2</sub>) and Silicon dioxide (SiO<sub>2</sub>) with Epoxy resins are combinedly used for fabrication in different types of FGM materials. Additionally, a particle has been added at high operating voltages to analyze the spacer's unfavourable behaviour, and the stresses have then been reduced by inserting metal pieces. The Glerekson's finite element approach is used to evenly distribute the field throughout a material composed of FGM and filler material of varying permittivity. The proposed spacer is simulated for different operating voltages (72.5kV, 132kV and 220kV) with delamination and particle as defects. By adding a metal insert (MI) to the post-type spacer, the effect of aluminium particles with delamination is decreased, and the findings are then presented and studied.

**Keywords**-Gas Insulated Busduct, Field, Spacer, Triple Junction (TJ), Metal Insert

### 1. INTRODUCTION

Gas Insulated Busduct (GIB) is widely used in today's high voltage applications as they are serving critical loads, essential to meet the high power demand and safety of the public.

Ideally, these substations are designed to avoid their failures from natural calamities like environmental changes, floods etc. Though GIB is more efficient than conventional substations, a few challenges are faced by them mainly due to failures of spacers. Due to abnormalities such as particle contamination, delamination, etc., insulating spacers lose their dielectric strength, hence a suitable approach must be used to reduce the electric stresses brought by these spacer failures.

The research on electric stresses in GIB and gas-insulated lines, which is crucial for the best energy allocation, has been done by several researchers in the literature [1]. Vikharev.A.P [2] have reviewed that the contamination of the different spacers like cone and disc type spacers resulted in dielectric strength loss which is further reduced by using the shape control method. T. Takuma et al. [3] investigations revealed that the shape of a spacer can be regulated by employing an efficient method of spacer geometry management, which facilitates a uniform field across the spacer surface. Aluminium oxide ( $Al_2O_3$ ) and epoxy materials have been suggested by various studies [4-6] as functionally graded material-type spacers in order to improve the dependability of GIS insulators. Heung-Jin Ju et.al [7], has studied that FGM spacers with various permittivity distribution are used for controlling the field distribution in GIS spacers in HV applications. However, this method can be used to construct the spacer in the GIB for better performance. The field distributions due to various flaws are to be explored under various surges. To create disk-type, coaxial-type solid insulators, N. Hayakawa et al. [8] invented an FGM process, manufactured them, and imitated U-FGM. Chakravorti. S et. al [9] discovered that the majority of electron emission occurs near the TJ and this decreases the field. Using finite element modeling (FEM), Chen, J et al. [10] examined how the FGM technique is used to grade the plain epoxy spacer with different permittivity values to reduce the field and get a more compact GIS.

Toigo, C et al. [11] noted that one of the factors contributing to the loss of electrical insulation, which results in a surface flashover in the GIS, is spacer failure. The crucial factor in finding and determining the likelihood of spacer failure is the field distribution along the spacer surface. Despite this, the spacer surface exhibits several additional defects, including delamination, cracks, particles, and vacancies.

Delamination is one of the key problems with the manufacturing process design for spacers, according to few authors [12, 13]. This defect results in partial discharge because it

affects other system characteristics, including spacer size, insulating gas, structure, the position of the defect, a form of the TJ, and residues with metallic particles. However, this unfavorable effect causes the GIB to fail, thus it must be managed. G. Ueta et. al [14] identified that spacers in GIS are insulation parts which affect the dielectric medium by deteriorating the life of the equipment by testing results of high voltage tests, and partial discharge (PD) tests in real-time factories. According to several researchers [15, 16], Ultra-high-frequency (UHF) Partial Discharge activity is the primary reason for GIS failure. This issue has arisen as a result of several defects and a variety of monitoring techniques. Because of its high sensitivity and anti-electromagnetic interference properties, optical sensing has recently gained popularity. This issue can be resolved by using a UHF external antenna sensor measurement system in conjunction with a variety of techniques that collect the PD signal. Polamraju V. S. Sobhan [17] has identified that the size of the particle leads to corona effect spacers. M. Talaat et al. [18] reviewed that the dielectric properties of free particles in cone type spacer are better than disc type spacer for the proposed FGM grading, and they examined that small spherical conducting particles (due to mechanical, isolator, and circuit breaker switching) disrupted the field distribution throughout the surface of the spacer. This analysis can be extended with post-type FGM, and further can be reduced by using MIs.

Several authors focused only on 1-phase GIS to investigate the electric stresses of various spacer types at the TJ's endpoints of the spacer due to either delamination or particle contamination. By changing the permittivity of the spacer, the FGM-type spacer is an innovative method for dropping overall electric stresses within GIS. One of the most common spacer faults is delamination, a gap formed between the enclosure ends and the spacer. Particles, which typically arise during manufacture or as a result of disturbances during three-phase GIB operation, are another fault that has been noted. Subcategories of these particles include conductive, dielectric, floating, and free.

This study uses an FGM post-spacer with various gradings to analyze the electric stresses at the TJ enclosure end in a three phase. The insulation qualities are tested for the field at the TJ enclosure end of the FGM spacer. A metallic particle is also added at this junction, along with the site of the electric strains brought on by either FGM Spacer delaminating at the TJ. To ensure a consistent field, a recessed Metal Insert can be put at the enclosure end of conductor Y by

shaping the metal to the enclosure end's shape. Analysis of the electric stresses at the TJ shows that for three various intervals of permittivity values, types of gradings of FGM at TJ of conductor Y, and permittivity values, the electric stresses deteriorate due to both the flaws at such a junction.

## 2. MATHEMATICAL MODELING OF GIB

Using the two key electrostatics equations, many researchers have estimated the electric field. The FEM, an effective technique for resolving issues with electric fields, is employed in this article to find out the electric stresses on the spacer surface.

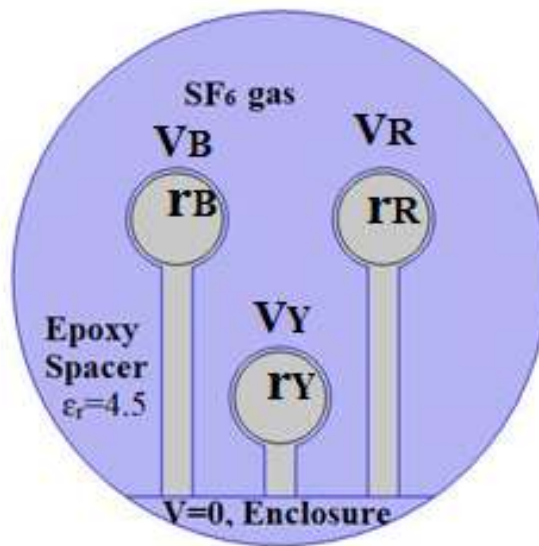


**Figure 1.** Boundary conditions three phase GIB

$$\vec{E} = -\nabla V \quad (1)$$

where, the potential is  $V$ .

From the concept of divergence theorem

$$\nabla \cdot \vec{D} = \rho_v \quad (2)$$

we know that flux density and field intensity are related as,

$$\vec{D} = \epsilon \vec{E} \tag{3}$$

Substituting Eq. (3) and Eq. (1) in Eq. (2),

$$\nabla \cdot \epsilon \vec{E} = \rho_v \tag{4}$$

$$\text{then, } \nabla \cdot \epsilon (-\nabla V) = \rho_v \tag{5}$$

then Eq. (5) is simplified into Poisson's equation, which is given by Eq. (6), for a linear, isotropic, and homogeneous system

$$\nabla^2 V = \frac{-\rho_v}{\epsilon} \tag{6}$$

The volume charge density  $\rho_v$  is zero if the charge is spread uniformly, hence Eq.(6) reduced to Laplace's equation, which is shown in Eq. (7) is zero, and hence Eq. (6) can be written to Laplace's equation as represented in Eq. (7)

$$\nabla^2 V = 0 \tag{7}$$

Following the principle of variation, the zero-derivative storage of energy is achieved by the following solution to the potential V,

$$\text{Hence } dW = 0 \tag{8}$$

### 3. FUNCTIONALLY GRADED MATERIAL

To create a uniform field along the length of the spacer, the FGM technique is utilized. Three different forms of grading are used with FGM methods in this paper: GL, GH, and GU. The manufacture of GL- FGM is shown in Fig. 2, and Table. 1's permittivity values are used to determine the values for various instances. Figure 3 depicts the variation of permittivity values for various FGM gradings for the permittivity variation of example 1.

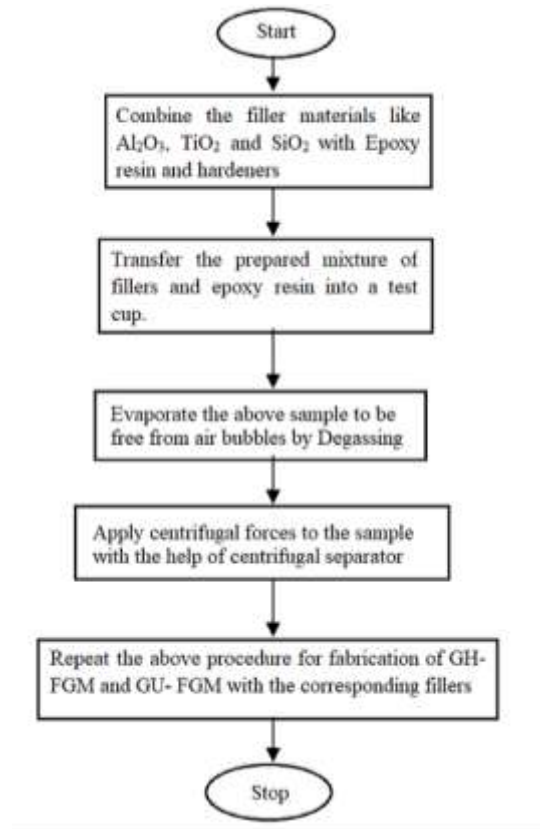


**Figure 2.**Flowchart for manufacturing GL-FGM

**Table 1.** Permittivity Grades for different FGM's

| Grading Type | Permittivity Ranges |                    |                    |
|--------------|---------------------|--------------------|--------------------|
|              | CaseA               | Case B             | Case C             |
| GL           | 3.95 - 3.50         | 4.05 - 3.60        | 4.15 - 3.70        |
| GH           | 3.50 - 3.95         | 3.60 - 4.05        | 3.70 - 4.15        |
| GU           | 3.95 -3.50 - 3.95   | 4.05 - 3.60 - 4.05 | 4.15 - 3.70 - 4.15 |

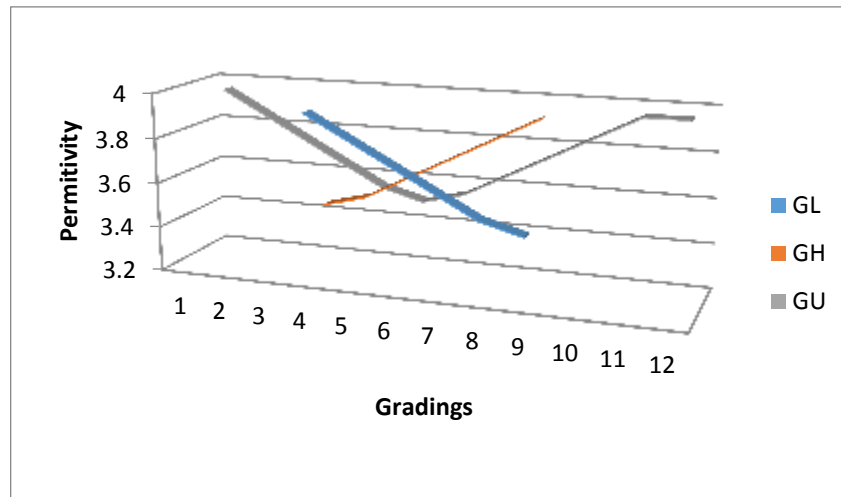


**Figure 3.** Case A permittivity ( $\xi$ ) variation of gradings

The 10 equal blends of the three conductors corresponding spacer lengths and widths are used in the construction of the FGM spacer. The above mentioned FGM techniques are used for the grading, each using a different spectrum of permittivity. For these three forms of grading, the FGM spacer is examined using the aforementioned cases and the corresponding permittivity ranges.

#### 4. RESULTS AND DISCUSSIONS: ELECTRIC STRESS REDUCTION DUE TO DELAMINATION AND PARTICLE WITH MI

Epoxy alumina is used as a spacer material and simulated using FEM analysis, as shown in Fig. 4 and three conductors placed at the equidistance from each other

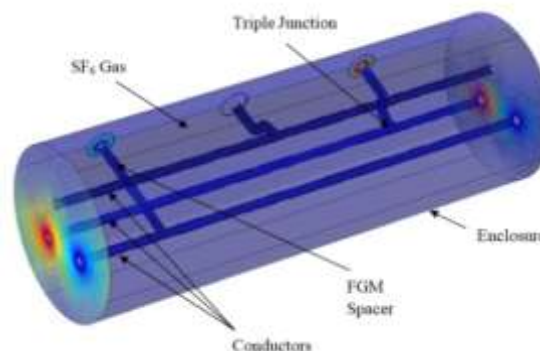


**Figure 4.3**-phase GIB design

Three conductors R, Y, and B are all kept in same enclosed GIB in the proposed simulation model at equal distances from one another. The voltages of the conductors VY and VB are applied to the conductor R and the RMS voltages of VR are 72.5 , 132 and 220 kV respectively. The enclosure end's outside electrode, which has no voltage, is grounded.

Figure 5 displays the design diagrams for the particle for FGM Post type with MI and the 3-phase GIB with delamination. A MI with various shapes and dimensions is observed to lessen the impact of delamination and particle effect on the FGM spacer. A suitable MI with the shape that has the maximum reduction in field is identified; consequently, this specific MI is utilized at the conductor Y. By inserting a MI at the enclosure end, additional electric strains on the FGM spacer are reduced. Fig. 5 depicts the planned Metal insert with the aforementioned dimensions.

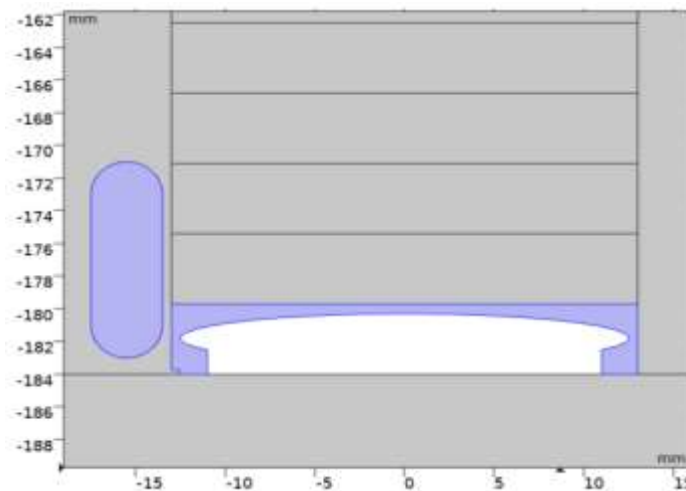


**Figure 5.** Particle with delamination micro defect and MI on FGM spacer

Metallic particle is present as another typical defect which occurs due to several operations, leading to the failure of Spacers and here the simulation of FGM spacer with delamination and particle together is done to investigate the field effect. The designed spacer resulted in high electric stresses at TJ of conductor Y is as in Table 2. Further, a MI is inserted at the TJ in the same conductor as shown in Fig. 5.

From Table 2, it can be seen that after inserting MI at conductor Y, Case C has a maximum reduction of 80.87 % of electric stresses at the TJs of the enclosure end at the 220KV operating voltage and for Case C of FGM grading, the reduction is around 82% at 72.5KV and for Case C



of GU grading the percentage reduction is observed as 81.93 % at 72.5 KV when compared to all other cases. Fig. 6 represents that the magnitude of Electric stresses at TJ of the enclosure end due to the particle is high and it is reduced by using MI at the TJs and the obtained results are shown in Fig. 7, It is observed clearly that the electric stresses are reduced from 0.2045 to 0.0392 KV/cm, 0.373 to 0.0715 KV/cm and 0.6222 to 0.119 KV/cm at 72.5 KV, 132KV and 200KV respectively as shown in the zoomed plots of Figs. 8 and 9.

**Table 2.** Electric stresses due to delamination with particle

| Type       | Permittivity<br>( $\xi$ ) | Electric stresses without MI in<br>KV/cm |               |               | Electric stresses with MI in<br>KV/cm |               |               |
|------------|---------------------------|--|---------------|---------------|---------------------------------------|---------------|---------------|
|            |                           | V1=<br>72.5KV                            | V2=<br>132 KV | V3=<br>220 KV | V1=<br>72.5KV                         | V2=<br>132 KV | V3=<br>220 KV |
| GL-<br>FGM | CaseA                     | 0.2042                                   | 0.3725        | 0.62          | 0.04023                               | 0.0735        | 0.1225        |
|            | CaseB                     | 0.2044                                   | 0.3727        | 0.62175       | 0.0397                                | 0.0722        | 0.1208        |
|            | CaseC                     | 0.2045                                   | 0.373         | 0.6222        | 0.0392                                | 0.0715        | 0.119         |
| GH-<br>FGM | CaseA                     | 0.186                                    | 0.339         | 0.5654        | 0.0346                                | 0.063         | 0.1054        |
|            | CaseB                     | 0.1864                                   | 0.34          | 0.5668        | 0.0342                                | 0.0624        | 0.1041        |
|            | CaseC                     | 0.1867                                   | 0.3406        | 0.568         | 0.0338                                | 0.0617        | 0.1029        |
| GU-<br>FGM | CaseA                     | 0.188                                    | 0.3427        | 0.5716        | 0.0349                                | 0.0638        | 0.10645       |
|            | CaseB                     | 0.1884                                   | 0.3435        | 0.5728        | 0.0345                                | 0.063         | 0.1052        |
|            | CaseC                     | 0.189                                    | 0.3441        | 0.574         | 0.03415                               | 0.0623        | 0.104         |

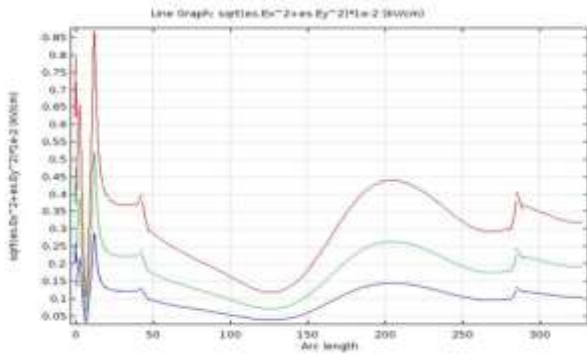


Figure 6. Effect of Delamination and Particle

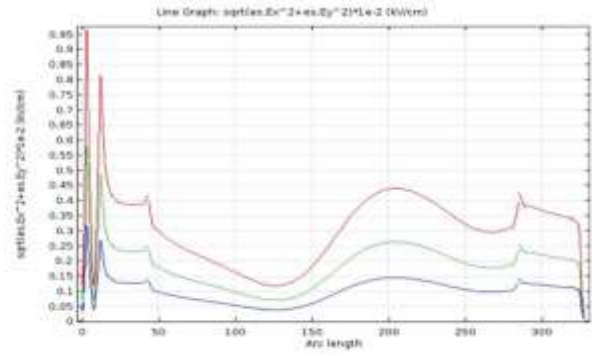


Figure 7. Reduction of Electric stresses with MI

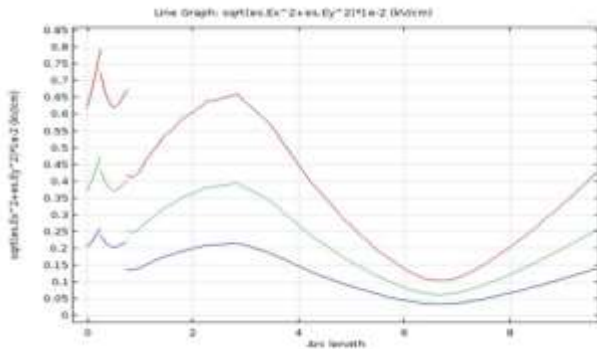


Figure 8. Zoomed Plot of spacer

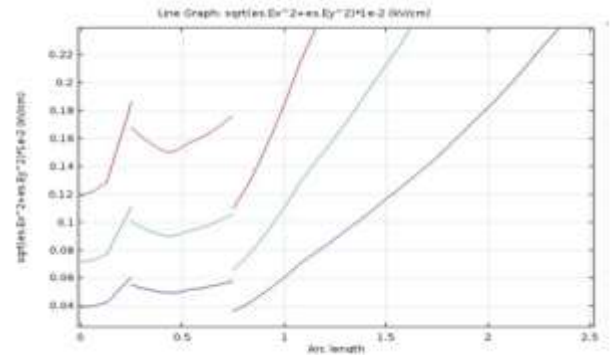


Figure 9. Reduced in electric stresses

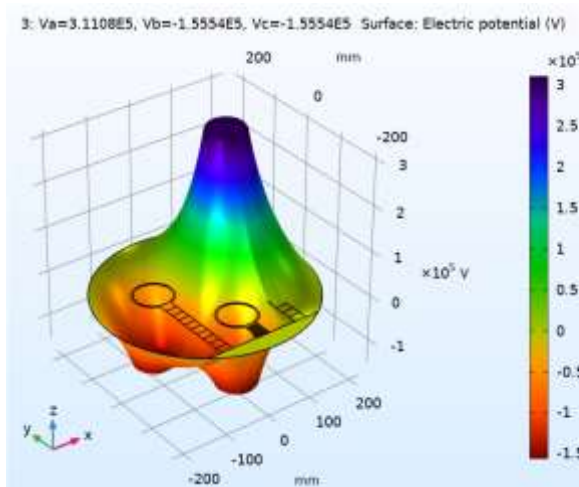


Figure 10. Surface Plot without MI

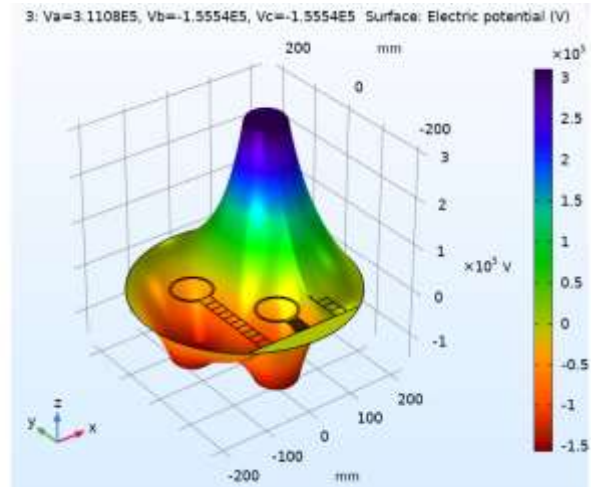


Figure 11. Surface Plot with MI

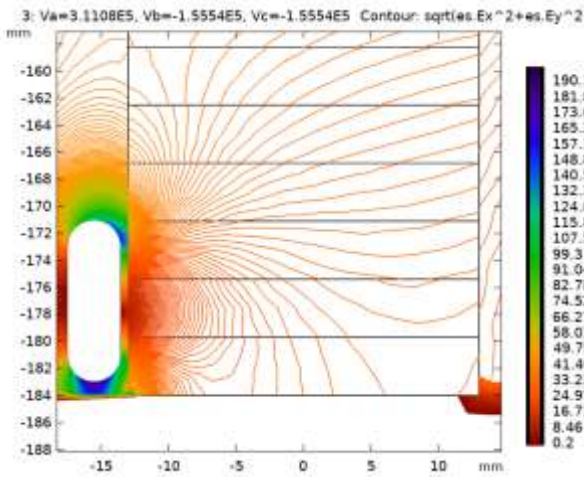


Figure 12. Contour Plot of Spacer

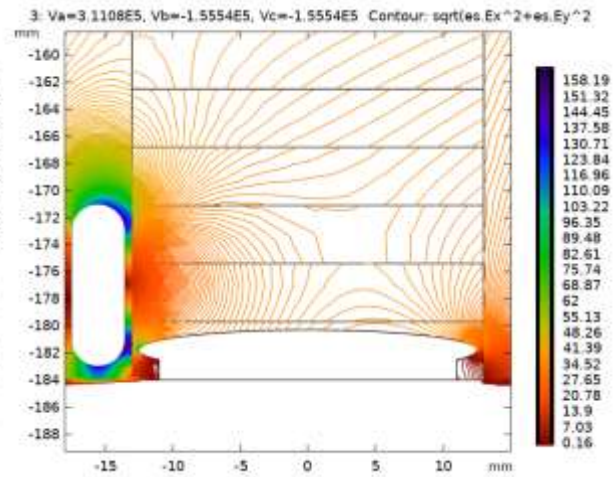


Figure 13. Contour Plot of Spacer with MI

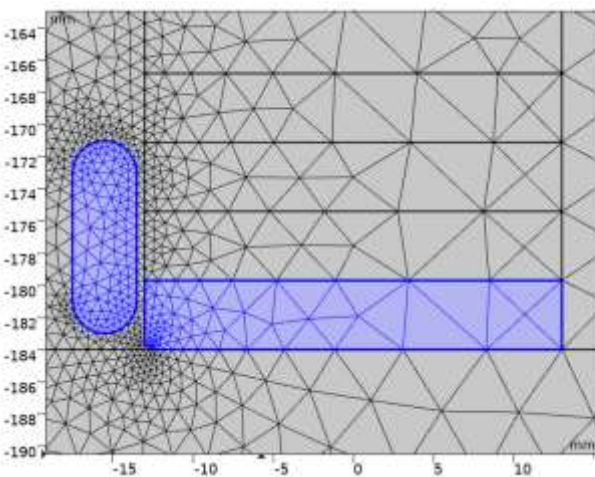


Figure 14. Mesh Plot of spacer

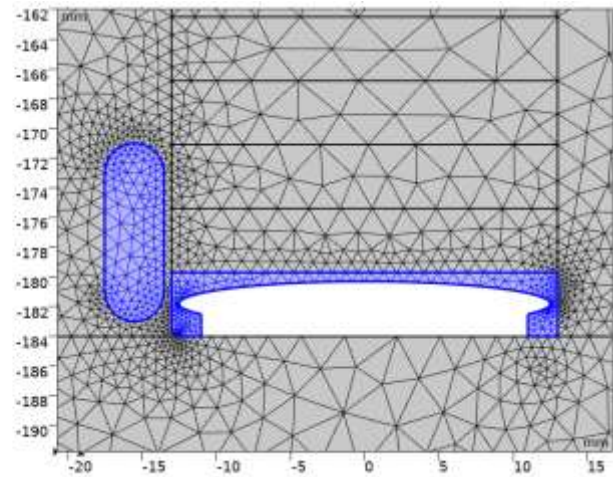


Figure 15. Mesh Plot of spacer with MI

Figures 10 and 11 use height as an axis to display surface plots of the FGM spacers with delamination and a particle introduced at Conductor Y without and with MI, respectively. In both figures, the blue height increases indicate where the stress is greatest relative to the other conductors; this is conductor R. Figures 12 and 13 depict the contour plot of a conductor for a conductor Y for a FGM Spacer and, as a result, a decrease in electric stresses with MI. High electrical field stress at particles and delamination is depicted by the thick blue lines.

Similarly, the Mesh plot shows the electric strains caused by Particle without and with MI in the planned FGM Spacers. Due to the field's curved shape, as seen in Figs. 14 and 15, the density

of the mesh infers that the field established is high. Mesh plots are mostly used to control plot element quality rather than colour. To produce the most exciting results, mesh plots are generated with various data sets for various plots and are displayed as a collection of single plots.

## **5. CONCLUSION**

The effect of delamination and particle is examined in this research for a three-phase GIB using an FGM Spacer, with conductor Y experiencing the highest electric strains at TJ when compared to the other conductors at various locations. Due to the prevalence of delamination and particle in high-voltage working GIBs, various sizes of delamination and various types of particles, including aluminium, copper, and silver, are used to illustrate these major flaws. Due to the fact that Conductor Y experiences disproportionately high electric stresses at TJ of the enclosure end, compared to all the Conductors of R, Y, and B. Both defects are introduced at the same conductor Y, and their impact has been lessened by adding a MI at TJ of the enclosure end of the spacer.

The proposed method has produced better results by using MI at TJ instead of well existing Shape control techniques of spacer. With this insertion of MI the electric field is redistributed and thereby reducing the stresses which inturn prevents the spacer from its insulation failure in GIB. When compared to other cases, GH FGM, and GU FGM gradings, Case C of GL- FGM has higher electric stresses for the fault delamination at the TJ of Conductor Y. The maximum field reduction is obtained for Case C of GU FGM when compared to all other cases by inserting a recessed MI at the TJ of the enclosure in three-phase GIB. This is because the defect delamination along with particles causes the field to be significantly worsened.

Although the electric field distribution is reduced significantly by using MI in this work, however still there is a scope to further reduce the stress by using different spacer models. This work can be carried out for different spacer designs and also can be analyzed for different defects like voids, depressions etc.

## **REFERENCES**

1. Shu.Y, Chen.W, “Research and application of UHV power transmission in China”, High Voltage, Vol.3 (1), pp. 1-13, 2018.

2. Vikharev.A.P , “Transmission Capacity of Gas-Insulated Power Lines Laid in Earthen Trenches”,Power Technology and Engineering,Vol. 53(1), pp.101-105,2019.
3. T. Takuma et.al,”Field behavior near singular points in composite dielectric arrangements”, IEEE Trans. Electr. Insul.,Vol.13, pp. 426-435,1978.
4. Liang.H, Du.B, Li.J, Wan.Z, “Mechanical stress distribution and risk assessment of 110 kV GIS insulator considering Al<sub>2</sub>O<sub>3</sub> settlement”, High Voltage, Vol.4 (1), pp. 65-71, 2019.
5. H.Okubo, J.Shimomura, Y.Fujii, N.Hayakawa, M.Hanai and K.Kato, “Fabrication and Simulation Techniques of Permittivity Graded Materials for Gas Insulated Power Equipment”, ISH, E-095, 2011.
6. Talaat, M., El-Zein, A., Amin, M., “Developed optimization technique used for the distribution of U-shaped permittivity for cone type spacer in GIS”, Electric Power Systems Research, 163, pp. 754-766, 2018.
7. Heung-Jin Ju, Bongseong Kim and Kwang-Cheol Ko, “Optimal Design of an Elliptically Graded Permittivity Spacer Configuration in Gas Insulated Switchgear”, IEEE Transactions on Dielectrics and Electrical Insulation, Vol.18(4),pp.1268- 1273,2011.
8. Naoki Hayakawa , Junya Ishiguro ,Hiroki Kojima , Katsumi Kato , Hitoshi Okubo, “Fabrication and Simulation of Permittivity Graded Materials for Electric Field Grading of Gas Insulated Power Apparatus”, IEEE Trans. on Dielectrics and Electrical Insulation, Vol. 23(1), pp. 547-554, 2016.
9. Chakravorti.S, A.Lahiri, “Electrode-Spacer Contour Optimisation by ANN aided Genetic Algorithm”, IEEE Trans. on Dielectrics and Electrical Insulation,Vol.11(6), pp. 964-975,2004.
10. Muneaki. K, Katsumi. K, Masahiro. H, Yoshikazu Hoshina , Masafumi Takei , Hitoshi Okubo, “Application of Functionally Graded Materialfor Reducing Electric Field on Electrode and Spacer Interface”, IEEE Transactions on Dielectrics and Electrical Insulation Vol. 17( 1), pp.256- 263 ,2010.
11. Chen, J., Xu, C., Li, P., Shao, X., Li, C., “ Feature Extraction Method for Partial Discharge Pattern in GIS Based on Time-frequency Analysis and Fractal Theory”, Gaodianya Jishu/High Voltage Engineering, 47 (1), pp. 287-295,2021.
12. Toigo, C., Vu-Cong, T., Jacquier, F., Girodet, A., “ Partial discharge behavior of protrusion on high voltage conductor in GIS/GIL under high voltage direct current: Comparison of SF<sub>6</sub>

- and SF6 alternative gases”, IEEE Transactions on Dielectrics and Electrical Insulation, 27 (1), art. no. 8985625, pp. 140- 147, 2020.
13. P. Janaki, N. Karthick, G.V. Nagesh Kumar, “ Design and analysis of FGM post type spacer in a three phase common enclosure gas insulated busduct under delamination”, Electric Power Systems Research, 190, pp. 1-23, 2021.
14. Genyo Ueta , Junichi Wada , Shigemitsu Okabe , Makoto Miyashita ,Chieko Nishida ,Mitsuhito Kamei,” Insulation Characteristics of Epoxy Insulator with Internal Crack-shaped Micro-defects - Study on the Equivalence of Accelerated Degradation by Frequency Acceleration Test”, IEEE Transactions on Dielectrics and Electrical Insulation, Vol. 21 (3), pp.1216- 1225, 2014.
15. Tanaka.H, Tanahashi.D, Baba.Y, Nagaoka.N, Okada.N, Ohki.H, Takeuchi.M, “ Finite-difference time-domain simulation of partial discharges in a gas insulated switchgear”, High Voltage, Vol.1(1), pp. 52-56, 2016.
16. Hong-Yang.Z, Guo-Ming.M, Wang.Y, Wei-Qi.Q, Jiang.J, Yan.C, Cheng-Rong.L, “Optical sensing in condition monitoring of gas insulated apparatus: A review”,High Voltage, Vol.4 (4), pp. 259-270,2019.
17. Polamraju V. S. Sobhan, Janaki Pakalapati, Venkata Nagesh Kumar Gundavarapu, Deepak Chowdary Duvvada, Sravana Kumar Bali., “Electric Field Stress in a Three Phase Common Enclosure Gas Insulated Busduct with FGM Post Type Spacer and Reduction with Metal Inserts”, Journal of Electrical Engineering & Technology, 16, pp. 985–1002, 2021.
18. M. Talaat, A.El-Zein , M. Amin, “Developed optimization technique used for the distribution of U-shaped permittivity for cone type spacer in GIS”, Electric Power Systems Research- Elsevier, Vol. 163, Part B, pp. 754-766,2017.